*Polish Journal of Chemical Technology, 18, **4**, 110—116, 10.1515/pjct-2016-0079*

Synthesis and antibacterial properties of Fe_3O_4-Ag nanostructures

Anna Pachla, Zofia Lendzion-Bieluń*, Dariusz Moszyński, Agata Markowska-Szczupak, Urszula Narkiewicz, Rafał J. Wróbel, Niko Guskos[1], Grzegorz Żołnierkiewicz[1]

West Pomeranian University of Technology, Szczecin, Institute of Chemical and Environment Engineering, Faculty of Chemical Technology and Engineering, ul. Pułaskiego 10, 70-322 Szczecin, Poland
[1]West Pomeranian University of Technology, Szczecin, Institute of Physics, ul. Pułaskiego 10, 70-322 Szczecin, Poland
Corresponding author: e-mail: zosi@zut.edu.pl

Superparamagnetic iron oxide nanoparticles were obtained in the polyethylene glycol environment. An effect of precipitation and drying temperatures on the size of the prepared nanoparticles was observed. Superparamagnetic iron oxide Fe_3O_4, around of 15 nm, was obtained at a precipitation temperature of 80°C and a drying temperature of 60°C. The presence of functional groups characteristic for a polyethylene glycol surfactant on the surface of nanoparticles was confirmed by FTIR and XPS measurements. Silver nanoparticles were introduced by the impregnation. Fe_3O_4-Ag nanostructure with bactericidal properties against Escherichia coli species was produced. Interesting magnetic properties of these materials may be helpful to separate the bactericidal agent from the solution.

Keywords: Fe_3O_4 nanoparticles, superparamagnetic nanoparticles, silver nanoparticles.

INTRODUCTION

Magnetic nanoparticles of Fe_3O_4 have brought an interest in recent years. Preparation of magnetite nanoparticles in a very narrow range of crystallite size, which exhibits superparamagnetic properties is of special interest. Superparamagnetic materials are characterised by an ultrafast response to changes of electromagnetic field[1, 2] and a lack of magnetic hysteresis arising due to the fact that a single particle is a separate monodomain and resemble a paramagnetic atom or ion[3, 4]. Superparamagnetic properties of Fe_3O_4 have found applications in medicine for drug transport as a local magnetic therapy, to diagnose and treat cancer using magnetic hyperthermia (ablation), for magnetic marking of cells (immunological separation) or for contrast strengthening in cell magnetic resonance imaging[5, 6].

The choice of preparation route of magnetic nanoparticles is dependent on their further application. The magnetic carriers in nanotechnology and medicine require a well-defined composition and size, high stability in aqueous conditions and lack of aggregation in organic as well as aqueous solvents in a wide range of pH[7]. The composition and dispersion stability is required regardless of a change of the ionic strength of a solution[8] and the presence of other substances[9]. Therefore multiple preparation methods of iron oxide (II)(III) was developed i.e.: precipitation[10], solvothermal[11], hydrothermal[12], microemulsion[13], thermal decomposition[12], sol – gel method[14], and liquid polyols[15].

A typical solovothermal[16, 17] synthesis of Fe_3O_4 consists in dissolution of $FeCl_3$ in polyethylene glycol and then addition of sodium acetate (NaAc). Such prepared solution is poured into a teflon vessel and placed in an autoclave. The solution heated up to 200°C is kept at these conditions for 8 hours and then cooled down to an ambient temperature. Prepared nanoparticles are separated with a magnet, washed out with alcohol, and dried at a temperature of 60°C for 10 hours. We can find many references with modifications of the described method. In work[18] authors added not only sodium acetate but also sodium citrate into iron salt solution in PEG.

The described preparation is a combination of a solvotheramal and a polyol method. The mechanism of the polyol reaction is still under study. Polyethylene glycol decomposing to acetaldehyde[19] can be a reducer to reduce $FeCl_3$ to Fe_3O_4. Temperature is a factor which influence on glycol reduction potential. Besides PEG can play a role of surfactant, inhibiting growth of particles and reducing interactions leading to agglomeration. In that way we can control morphology of being synthesised particles. The surface of the prepared magnetite nanoparticles is coated with hydrophylic polyol ligands, therefore, the nanoparticles can be easily dispersed in a polar solvent.

Impregnation of nanomagnetic particles with silver, which exhibits antibacterial properties, increases the functionality of both materials and makes their application wider. It was found that silver antibacterial effectiveness is stronger when it is bound with Fe_3O_4[7]. Ag/Fe_3O_4 nanoparticles of core-shell type show antibacterial properties against such bacterial strains as *Escherichia coli, Staphylococcus epidermidis, and Bacillus subtilis*. Thanks to paramagnetic properties, nanoparticles may be easily separated from liquids, recycled, and reused[20]. Therefore they may have potential applications as water disinfection agents.

Considering preparation based on precipitation, one- and two-stage processes can be used to synthesise Ag/Fe_3O_4 nanoparticles. In the one-stage synthesis silver nitrate is added to an ethylene glycol solution (EG) containing iron (III) chloride, polyvinylpyrrolidone (PVP), and sodium acetate. A suspension of AgCl and Fe^{3+} cations in EG is formed. Then a thermal reaction at 180–200°C is carried out in an autoclave[21]. In the two-stage method, Fe_3O_4 is initially prepared and coated with silver. Glucose may be used as a mild reducer to coat magnetic nanoparticles of iron (II)(III) oxide with a silver layer. A solution containing Fe_3O_4, $AgNO_3$, and glucose in a molar ratio of 1:2:1 is sonicated for 15 minutes, heated in a water bath and slowly stirred for 1 hour. Finally the magnetic nanoparticles of Ag/Fe_3O_4 are separated with a magnet[22].

The main goal of the present study was an optimisation of the synthesis method of nanocrystalline Fe_3O_4 and Fe_3O_4-Ag composites. In this work a simple co-precipitation method in alkaline environment was used to obtain

nanocrystalline Fe_3O_4. Stoichiometric ratio of Fe^{2+}/Fe^{3+} ions equal 0.5 was applied. In order to control size of being formed particles an environment polyethlene glycol, which protects against agglomeration, was used. The influence of precipitation and drying temperatures on the size of Fe_3O_4 crystallites was examined. Nanostructure of Fe_3O_4-Ag was prepared in a two-stage process by impregnation of nanoparticles of Fe_3O_4 oxide. Polyethyleimine (PEI) was used as a mild reducer of $AgNO_3$ and a binder of silver over the surface of Fe_3O_4 nanoparticles. The ramified chain of PEI has a high density of amine groups[23], which are used to stabilise various inorganic forms of nanoparticles e.g. gold[24]. The antibacterial properties of Fe_3O_4-Ag composites was also determined.

PREPARATION AND CHARACTERIZATION

Synthesis of Fe_3O_4 nanoparticles

Nanoparticles of iron oxide (II, III) were obtained by the precipitation method. 0.420 g of iron chloride (II) and 0.840 g of iron chloride (III) were dissolved in 40 ml of distilled water. Next, 40 ml of polyethylene glycol was added and the solution was stirred (500 rpm) in an inert atmosphere (N_2). When slowly heated mixtures reached 80°C or 85°C, batching of 1-molar sodium carbonate solution was started. Sodium carbonate was added to reach a pH value of 10. The mixtures were cooled down to an ambient temperature and the magnetic Fe_3O_4 nanoparticles were separated by decantation with the aid of a magnet. The particles were rinsed with ethanol and distilled water and dried at 100°C or 60°C.

Synthesis of Fe_3O_4-Ag nanostructures

Silver was added to Fe_3O_4 nanoparticles by a wet impregnation. Silver nitrate (V) concentration was fixed to obtain mass ratio Ag:Fe_3O_4 = 1:100. The mixture of nanocrystalline Fe_3O_4 and silver nitrate (V) was sonicated twice for 15 min. Next, the water solution of 50% polyethyleimine (PEI, mild reducing agent) was added to the mixture and the whole of reagents was sonicated twice for 15 min. again. The suspension was filtered and the deposit was rinsed with alcohol and distilled water then dried at 60°C for 10 hours.

Characterization of prepared materials

A phase composition and an average size of Fe_3O_4 and silver crystallites were determined by powder XRD analysis with the aid of X'Pert Pro apparatus (Philips). A copper anode emitting CuKα radiation was applied. X'Pert HighScore software was used to identify crystallographic phases. The average size of crystallites was calculated from Scherrer's equation. A topography of the obtained Fe_3O_4 and Fe_3O_4-Ag was made with an electron scanning microscope (SEM) Hitachi SU-8800 and an EDX analyser was used to determine silver concentration. Specific surface area was determined on the basis of the BET method measurement of nitrogen adsorption-desorption isotherm using a Quadrasorb volumetric apparatus (Quantachrome Instrument). Pore volume was evaluated by the DFT method using QuadraWin software.

The X-ray photoelectron spectra were obtained using Al *Kα* (h = 1486.6 eV) radiation with a Prevac system equipped with Scienta SES 2002 electron energy analyser. The surface composition of the samples was calculated on the basis of the peak area intensities using the sensitivity factor approach and assuming homogeneous composition of the surface layer. The charging effects were corrected by setting the main component of C 1s transition at the binding energy of 285.0 eV. The functional groups present on the surface of nanocrystalline Fe_3O_4 and Fe_3O_4-Ag particles were determined by FTIR analysis using Thermo Scientific Nicolet 380 equipment. Magnetic properties of Fe_3O_4 and Fe_3O_4-Ag nanoparticles were determined with the aid of SQUID (MPMS – SQUID – XL – 7AC) magnetometer.

Escherichia coli strain K12 (ACCT 25922) was used as test organisms. The bacteria were first incubated in Nutrient Broth (Biocorp, Poland) at 37°C until a level of approximately 10^8 CFU/ml was reached (0.5 in McFarland standard, BioMérieux, France). Then 100μl of bacterial suspension was added to 10 ml saline solution (0.9% NaCl) containing different concentrations of Ag-FeO_3 nanocomposites and then incubated at 37°C (incubator with a controlled temperature and humidity) with continuous agitation (150RPM). After 3, 6 and 24 hours the antibacterial efficacy was determined by serial dilution method. The appropriate dilutions in NaCl solution (0.9%) were plated on Plate Count Agar (Biocorp, Poland) and incubated for 24 hours at 37°C. Then the colony forming units (CFU/ml) were counted. The experiment was verified three times.

RESULTS AND DISCUSSION

Several various factors may influence on the formation process of nanocrystalline iron oxide(II, III) and its composite with silver. Three samples of iron oxide were produced in the processes with varied parameters: precipitation temperature and drying temperature.

Phase compositions of prepared samples were examined by X-ray diffraction. Diffraction patterns denoted Fe_3O_4-1 and Fe_3O_4-2, made for materials precipitated at 80°C and dried at 100°C and 60°C, respectively, are shown in Figure 1. The peaks located at angular positions of 30.1° (220), 35.5° (311), 43.1° (400), 53.4° (422), 57.1° (511), and 62.8°, observed in both patterns, correspond to spinel structure of Fe_3O_4 (ICDD No. 88-0315). They confirm that the product contains only iron oxide(II, III) without any other iron oxides or other impurities. Detailed analysis of the diffraction peaks revealed a significant variation of their width between the samples (see insert in Fig. 1). Peak broadening was applied to calculate the average size of the Fe_3O_4 crystallites. In agreement with the changes of crystallite size, there is a change of the specific surface area measured for these samples. The results are shown in Table 1.

The optimal structural properties of the iron oxide(II, III) were obtained for precipitation temperature of 80°C and drying temperature of 60°C. This sample consists of the smallest crystallites (average crystallite size is 15 nm) and has the highest specific surface area (96 m^2/g). Higher precipitation temperature, 85°C instead of 80°C, results in the formation of slightly bigger crystallites

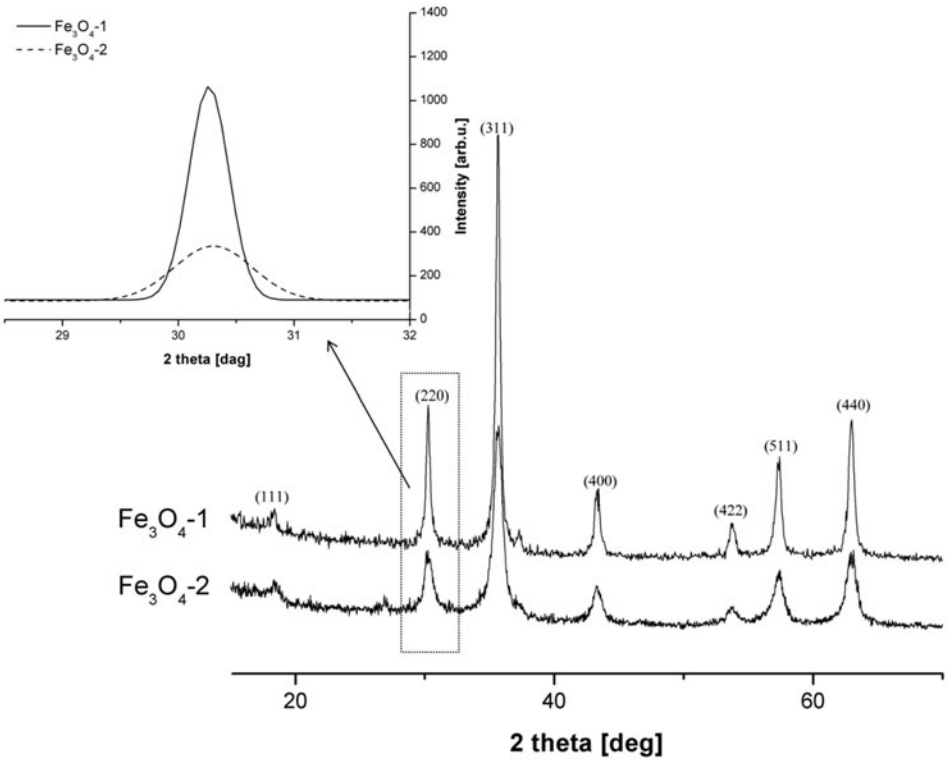

Figure 1. Schematic diagram of urea-based SNCR process kinetics[15]

Table 1. Precipitation and drying temperature, average size of crystallites, specific surface area, and pore volume of Fe_3O_4

Sample name	Drying temperature [°C]	Batching temperature of Na_2CO_3 [°C]	Crystallite sizes of Fe_3O_4 [nm]	Specific surface area [m^2/g]	Pore volume [cm^3/g]
Fe_3O_4-1	100	80	89.6	56.3	0.273
Fe_3O_4-2	60	80	15.2	96.3	0.314
Fe_3O_4-3	60	85	31.1	82.4	0.337
Fe_3O_4-Ag	60	80	14.7	97.3	0.376

(around 30 nm) and in effect smaller specific surface area (82 m^2/g). An increased drying temperature had the most detrimental effect on the formation of Fe_3O_4 nanocrystallites; a temperature of 100°C results in the formation of six times bigger Fe_3O_4 crystallites than those obtained at 60°C. Therefore the iron oxide(II, III) – Ag composite used in the further studies was prepared at the precipitation temperature of 80°C and was dried at 60°C. Impregnation of iron oxide with silver nitrate results in a slight decrease in the average crystallite size and correspondingly the specific surface area is higher (see Table 1). The sonication process during an impregnation stage may have influenced on the size of nanoparticles of Fe_3O_4.

The comparison of X-ray diffraction patterns of magnetite and Fe_3O_4-Ag nanostructure are shown in Figure 2. Peaks characteristic for the Fe_3O_4 phase are observed in both patterns. Additional peaks, at angular positions 38.1° (111), 44.3° (200), 64.4° (220), and 77.4° (311), are attributed to metallic silver (ICDD No. 87-0717). This is a proof that silver salt was reduced to metal and successfully introduced into the iron oxide substrate. The average size of silver crystallites is relatively high and amounts to around 36 nm.

Scanning microscopy images, Figure 3, show the structure of iron oxide (Fe_3O_4) and iron oxide covered with silver (Fe_3O_4-Ag). The average size of the particles estimated by the microscopic method is about 20 nm for both examined materials. This size is in good agreement

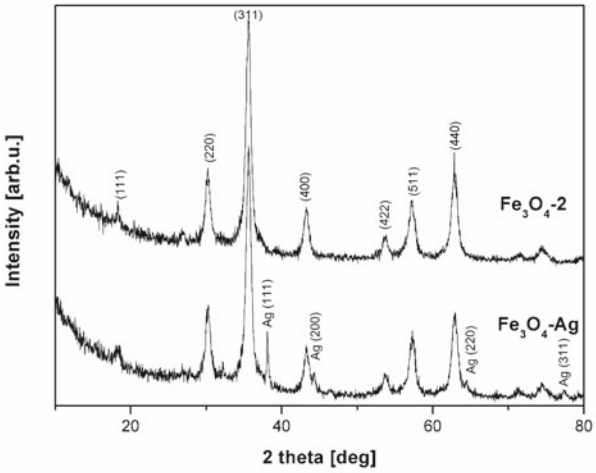

Figure 2. X-ray patterns of Fe_3O_4 and Fe_3O_4-Ag

with XRD evaluations for Fe_3O_4 formed in the optimal conditions. A statistical histogram of the fine particles showing a gain in percentage of 16–17 nm particles in the Fe_3O_4-Ag sample is worth to notice. The silver content in the sample Fe_3O_4-Ag was measured by EDS analysis and was about 0.4 atom % (1.3 wt.%).

The composition of the sample modified with silver was also examined by means of X-ray photoelectron spectroscopy. The XPS survey spectrum acquired for that sample is shown in Figure 4. Iron, oxygen, nitrogen, carbon, and silver atoms were identified. The concentra-

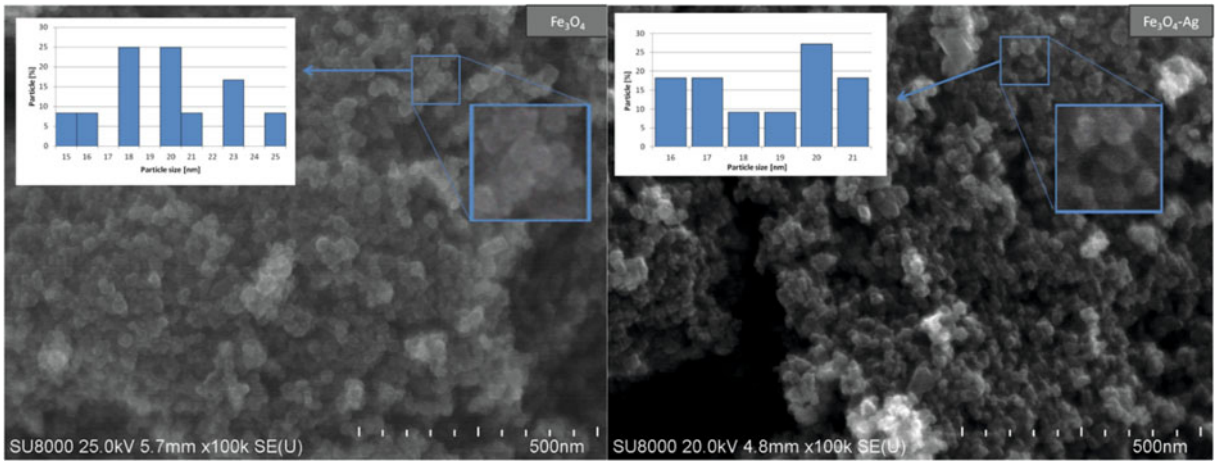

Figure 3. SEM images of Fe_3O_4 and Fe_3O_4-Ag

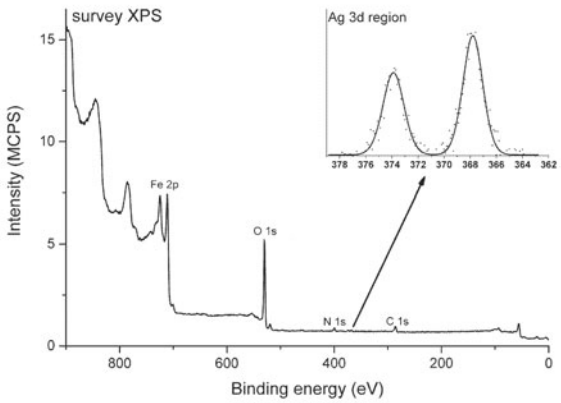

Figure 4. XPS survey spectrum of the sample Fe_3O_4-Ag. A region of Ag 3d transition is magnified

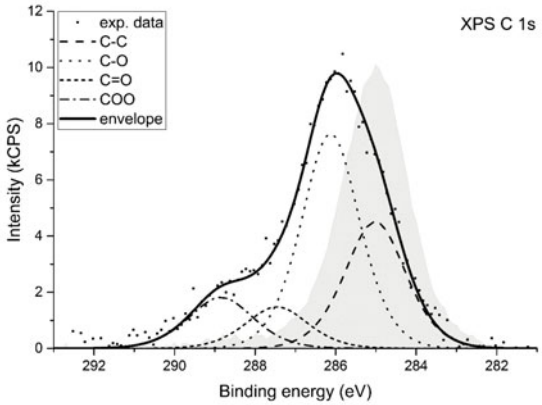

Figure 5. XPS C 1s transition for Fe_3O_4 sample produced by precipitation

tion of silver atoms calculated assuming a homogeneous distribution of all elements in a near-surface region is 0.3 at.% (about 1 wt.%). This value is consonant with EDS analysis mentioned above. The position of the maximum of Ag 3d line is 367.9 eV and corresponds well with the value characteristic for metallic silver.

During the preparation procedure, an organic surfactant in a form of polyethylene glycol is used. On the examined surface about 15 at.% of carbon was identified. An estimation of carbon layer thickness was carried out with a use of XPS Quant software[25]. The thickness obtained from that calculation is about 0.2 nm what can be interpreted as a submonolayer coverage of iron oxides by organic compounds.

The chemical state of the organic layer was investigated by the analysis of high-resolution XPS spectrum of C 1s transition (see Fig. 5). A common phenomenon is the presence of the adventitious carbon on the surface of inorganic samples examined with use of XPS. Therefore in Figure 5 XPS C 1s line acquired for magnetite obtained without organic surfactant is shown as a shaded area. There is a significant shift between the spectrum of the organic film on Fe_3O_4 and the adventitious carbon. The maximum of XPS C 1s peak is located at the binding energy of 286.0 eV.

The C 1s spectrum of the present sample was numerically deconvoluted into four components shown as thin lines below the envelope of XPS data. Considering components from the lowest binding energy one can attribute the given peak to the following chemical bindings of carbon atoms: position 285.0 eV is attributed to non-functionalized sp^3 carbon atoms (denoted C-C); position 286.1 eV is ascribed to a group of differently bonded carbon atoms linked to one atom of oxygen i.e. the functional groups as C-O-C or C-OH; position 287.5 corresponds to functional groups as C=O or O--C-O; position 288.8 eV is attributed to carbon atoms indicated by asterisk in the functional groups like C-O--C*=O or HO-C*=O. The binding energy assignments described above are based on the energy shifts given in Appendix E of Ref.[26].

The highest intensity is noted for the component ascribed to C-O-C bindings. In polyethylene glycol used as a surfactant during preparation stage, it is the main chemical environment of carbon atoms bound with oxygen atoms. The abundance of the C-O-C groups on the surface of the studied material is regarded as a prove of the successful deposition of the surfactant on the surface of iron oxides.

In polyethylene glycol, the chemical bindings between two carbon atoms are also present. Indeed the second most intense component of C 1s spectrum is located at 285.0 eV and corresponds with non-functionalized sp^3 carbon atoms. Apart from these two components, two other chemical environments were required to complete the deconvolution. They are ascribed to carbonyl and carboxyl groups, respectively. Despite these functional groups are not found in the polyethylene glycol struc-

ture their presence on the surface can be explained by a partial reconstruction of the bindings in the surfactant in the presence of iron oxides. It was already shown that iron oxides are good catalysts for alcohol oxidation[27].

Additional analysis of the surface components was performed by FTIR method. FTIR spectra of the Fe_3O_4 and Fe_3O_4-Ag nanostructures are shown in Figure 6. The wide band with a maximum at 3400 cm^{-1} may be attributed to the stretching vibration of the O-H group. Glycol, playing the role of surfactant protecting iron oxide particles against agglomeration, was a source of hydroxyl groups The characteristic stretching band of Fe-O is located at the position of 620 cm^{-1} [28]. In the range from 750 to 1350 cm^{-1} there is the wide band, which may be attributed to stretching vibrations of O-H and C-O-H[29]. The band is more intensive against a background of the nanostructure, what may be caused by additional C-N stretching vibrations[19]. The C-N stretching vibrations are characteristic for aliphatic amines and occur in the range of 1020–1250 cm^{-1}. The presence of these groups results from the PEI application during impregnation stage. The absorption peak at 1630 cm^{-1} may be imputed to

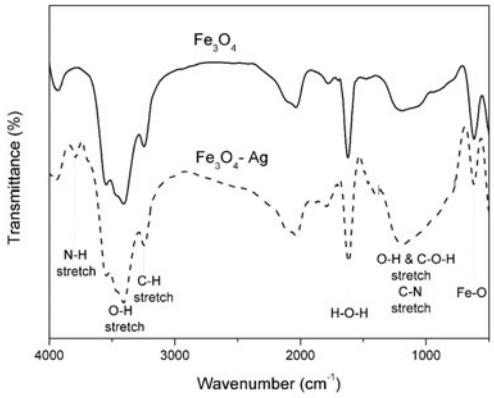

Figure 6. FTIR spectra of iron oxide and iron oxide with silver

benching vibrations of H-O-H bond in water molecules adsorbed on the surface of Fe_3O_4 and Fe_3O_4-Ag.

Magnetic properties of the nanocrystalline iron oxide and the Fe_3O_4-Ag composite were studied with a magnetometer with vibrating sample (a maximum applied field of 70 kOe) at ambient temperature. The hysteresis loops of Fe_3O_4 and Fe_3O_4-Ag are presented in Figure 7. Values characterising magnetic properties of the studied samples, namely magnetic coercivity, magnetic saturation (M_s), magnetic remanence (M_r), and reduced magnetic remanence (M_r/M_s) are given in Table 2. Magnetic saturation (M_s) of Fe_3O_4 nanoparticles of 56 emu/g is typical for magnetic nanoparticles synthesised by precipitation method[17, 30]. The presence of the silver (diamagnetic) decreases magnetic saturation to the value of 50.8 emu/g. It was found in the literature[31] that magnetic saturation of the magnetite bulk phase is about 92 emu/g. These differences are caused by a few factors, among others

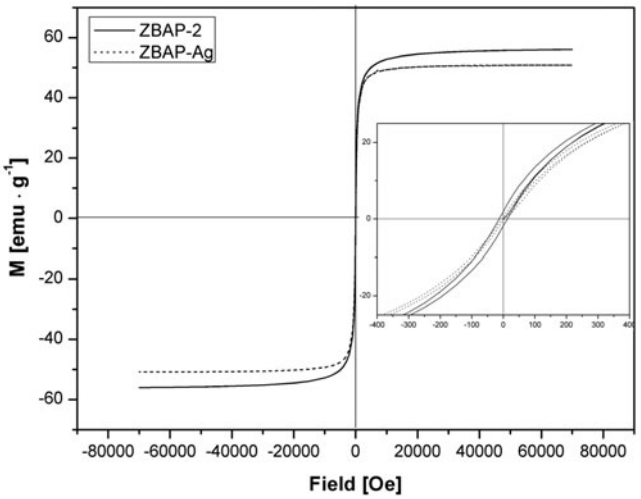

Figure 7. Magnetization curves as the function of magnetic field of Fe_3O_4 and Fe_3O_4-Ag

the presence of a surfactant on the surface[32, 33] which leads to decrease in the effective magnetic moment. Additional coverage with silver weakens magnetisation intensity further. The Fe_3O_4 is characterised by a small magnetic remanence value (M_r), which diminishes for the Fe_3O_4-Ag nanostructures.

The obtained results indicate that the samples are characterised by superparamagnetic properties and they can be easily separated from the reaction sludge with the aid of an external magnetic field.

The best antibacterial properties Fe_3O_4-Ag were found for the concentration of 120 μg/ml (see Fig. 8). Barely after 3 hrs, all bacteria was removed from saline solution. After 6 hrs viable *E. coli* was observed only in tubes containing Fe_3O_4-Ag at concentration of 40 μg/ml. A similar characteristic of nanocomposites containing silver has been demonstrated by other authors. Prucek at al[34] have shown that for Ag@Fe(3)O(4) and γ-Fe(2) O(3)@Ag a minimum inhibition concentration (MIC) was in the range from 15.6 mg/L (μg/ml) to 125 mg/L (μg/ml). Antiseptic properties of silver ions and silver based compounds have been well known[35–37].

On the basis of the obtained results we can state that a modification of Fe_3O_4 nanoparticles with silver leads to obtaining a nanostructure with antibacterial activity.

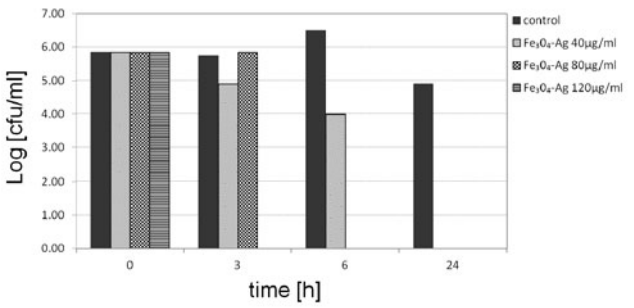

Figure 8. Bactericidal properties of Fe_3O_4-Ag for different amount of the sample in the saline (10 ml) after 3 hrs, 6 hrs, and 24 hrs

Table 2. Magnetic properties of Fe_3O_4 and Fe_3O_4-Ag

Sample	Coercivity [Oe]	M_s [emu/g]	M_r [emu/g]	M_r/M_s
Fe_3O_4	14	56.0	1.86	0.033
Fe_3O_4-Ag	7.0	50.8	0.43	0.008

CONCLUSION

The simple method of the preparation of magnetic Fe_3O_4 nanoparticles without a use of sophisticated equipment and complicated procedures was proposed. In comparsion with Fe_3O_4 polyol synthesis methods described in the literature we used significantly lower temperature and shorter reaction time to synthesised nanoparticles of Fe_3O_4.

The Fe_3O_4 nanoparticles can be further efficiently enriched with silver by impregnation. The Fe_3O_4-Ag nanostructures have good bactericidal properties. Additionally, the material demonstrated interesting magnetic properties which are helpful to separate the bactericidal agent from the solution.

LITERATURE CITED

1. Xu, C. & Sun, S. (2007). Monodisperse magnetic nanoparticles for biomedical applications, polymer international. Polym. Int. 56(7), 821–826. DOI: 10.1002/pi.2251.

2. Leem, G., Sarangi, S., Zhang, S., Rusakova, I., Brazdeikis, A., Litvinov, D. & Lee, T.R. (2009). Surfactant-controlled size and shape evolution of magnetic nanoparticles. Cryst. Growth Des. 9(1), 32–34. DOI: 10.1021/cg8009833.

3. Chełminiak, D., Ziegler-Borowska, M. & Kaczmarek, H. (2015). Nanocząstki magnetytu powlekane polimerami do zastosowań biomedycznych Cz. II. Nanocząstki Fe_3O_4 z powłokami z polimerów syntetycznych. Polimery, 60(2), 87–94. DOI: 10.14314/polimery.2015.087.

4. Pikul, A.P. (2012). Wybrane zagadnienia z fizyki magnetyków. Wrocław. Uniwersytet Wrocławski.

5. Gupta, A.K. & Guptab, M. (2005). Synthesis and surface engineering of iron oxide nanoparticles for biomedical applications. Biomaterials 26(18), 3995–4021. DOI: 10.1016/j.biomaterials.2004.10.012.

6. Fang, W., Zheng, J., Chen, C., Zhang, H., Lu, Y., Mac, L. & Chen, G. (2014). One-pot synthesis of porous Fe_3O_4 shell/silver core nanocomposites used as recyclable magnetic antibacterial agents. J. Magn. Magn. Mater. 357, 1–6. DOI: 10.1016/j.jmmm.2014.01.024.

7. Chen, Y., Gao, N. & Jiang, J. (2013). Surface matters: enhanced bactericidal property of core–shell Ag–Fe_2O_3 nanostructures to their heteromer counterparts from one-pot synthesis. Small 9, 3242–3246. DOI: 10.1002/smll.201300543.

8. Brollo, M.E.F., López-Ruiz, R., Muraca, D., Figueroa, S. J.A., Pirota, K.R. & Knobel, M. (2014). Compact Ag@Fe_3O_4 core-shell nanoparticles by means of single-step thermal decomposition reaction. Sci. Rep. 4, 6839. DOI: 10.1038/srep06839.

9. Chełminiak, D., Ziegler-Borowska, M. & Kaczmarek, H. (2015). Nanocząstki magnetytu pokryte polimerami do zastosowań biomedycznych. Cz. I. Otrzymywanie nanocząstek Fe_3O_4 z powłokami z polisacharydów. Polimery 60(1), 12–17. DOI: 10.14314/polimery.2015.012.

10. Hariani, P.L., Faizal, Ridwan, M. & Marsi, Setiabudidaya, D. (2013). Synthesis and properties of Fe_3O_4 nanoparticles by co-precipitation method to removal procion dye. Int. J. Environ. Sci. Dev. 4(3), 336–340. DOI: 10.7763/IJESD.2013.V4.366.

11. Yana, H., Lipinga, Z., Weiweia, H., Xiaojuanb, L., Xiangnongc, L. & Yuxianga, Y. (2010). A Study on synthesis and properties of Fe_3O_4 nanoparticles by solvothermal method. Glass. Phys. Chem+ 36(3), 325–331. DOI: 10.1134/S1087659610030090.

12. Lu, A.H., Salabas, E.L. & Schth, F. (2007). Magnetic nanoparticles: synthesis, protection, functionalization, and application. Angew. Chem. Int. Edit. 46(26), 1222–1244. DOI: 10.1002/anie.200602866.

13. Pérez, J.A.L. & Quintela, M.A.L. (1997). Advances in the preparation of magnetic nanoparticles by the microemulsion method. J. Phys. Chem. B 101(41), 8045–8047. DOI: 10.1021/jp972046t.

14. Kornak, R., Nižňanskỳ, D., Haimann, K., Tylus, W. & Maruszewsk, K. (2005). Synthesis of magnetic nanoparticles via the sol-gel technique. Mater. Sci. PL 23(1), 87–92.

15. Cai, W. & Wan, J., (2007). Facile synthesis of superparamagnetic magnetite nanoparticles in liquid polyols. J. Coll. Interf. Sci. 305, 366–370. DOI: 10.1016/j.jcis.2006.10.023.

16. Deng, H., Li, X., Peng, Q., Wang, X., Chen, J. & Li, Ya., (2005), Monodisperse Magnetic Single-Crystal Ferrite Microspheres. Angew. Chem. Int. Ed. 117, 2842–2845.

17. Xin, T., Ma, M., Zhang, H., Gu, J., Wang, S., Liu, M. & Zhang, Q. (2014). A facile approach for the synthesis of magnetic separable Fe_3O_4@TiO_2, core–shell nanocomposites as highly recyclable photocatalysts. Appl. Surf. Sci. 288(1), 51–59. DOI: 10.1016/j.apsusc.2013.09.108.

18. Tan, L., Zhang, X., Liu, Q., Jing, X., Liu, J., Song, D., Hu, S., Liu, L. & Wang, J. (2015) Synthesis of Fe_3O_4@TiO_2 core-shell magnetic composites for highly efficient sorption of uranium(VI). Coll. Surf. A. 469, 279–286. DOI: 10.1016/j.colsurfa.2015.01.040.

19. Ghazanfari, M., Johar F. & Yazdani, A. (2014). Synthesis and characterization of Fe_3O_4@Ag core-shell: structural, morphological, and magnetic properties. J. Ultrafine Grained Nanostruct. Mater. 118(47), 97–103.

20. Gong, P., He, H., Li, X., Wang, K., Hu, J., Tan, W., Zhang, S. & Yang, X. (2007). Preparation and antibacterial activity of Fe_3O_4@Ag nanoparticles. Nanotechnology 18(28). DOI: 10.1088/0957-4484/18/28/285604.

21. Zhang, D.H., Li, G.D., Lia, J.X. & Chen, J.S. (2008). Received one-pot synthesis of Ag–Fe_3O_4 nanocomposite: a magnetically recyclable and efficient catalyst for epoxidation of styrene. Chem. Commun. 29, 3414–3416. DOI: 10.1039/B805737K.

22. Moosavi, R., Afkhami, A. & Madrakian, T. (2015). A Simple cyanide sensing probe based on Ag/Fe_3O_4 nanoparticles. Anal. Chem. 5, 15886–15891. DOI: 10.1039/C4RA14806A.

23. Jäger, M., Schubert, S., Ochrimenko, S., Fischer, D., & Schubert, U.S. (2012). Branched and linear poly(ethylene imine)-based conjugates: synthetic modification, characterization, and application. Chem. Soc. Rev. 41, 4755–4767. DOI: 10.1039/C2CS35146C.

24. Wang, S.T., Yan, J.C. & Chen, L. (2005). Formation of gold nanoparticles and self-assembly into dimer and trimer aggregates. Mater. Lett. 59, 1383–1386. DOI: 10.1016/j.matlet.2004.12.045.

25. Mohai, M. (2006). XPS MultiQuant: a step towards expert systems. Surf. Interf. Anal. 38(4), 640–643. DOI: 10.1002/sia.2198.

26. Briggs, D., Grant, J.T. (2003). Surface analysis by auger and X-ray photoelectron spectroscopy in IM Publications and SurfaceSpectra Limited. Charlton Manchester.

27. Sadri, F., Ramazani, A., Massoudi, A., Khoobi, M., Tarasi, R., Shafiee, A., Azizkhani, V., Dolatyari, L. & Joo, S.W. (2014). Green oxidation of alcohols by using hydrogen peroxide in water in the presence of magnetic Fe_3O_4 nanoparticles as recoverable catalyst. Green Chem. Lett. Rev. 7(3), 257–264. DOI: 10.1080/17518253.2014.939721.

28. Li, C., Tan, J., Fan, X., Zhang, B., Zhang, H. & Zhang, Q. (2009). Magnetically separable one dimensional Fe_3O_4/P(MAA-DVB)/TiO2 nanochains: preparation, characterization and photocatalytic activity. Polymer 50, 1887–1894. DOI: 10.1016/j.ceramint.2014.11.064.

29. Shameli, K., Ahmad, M.B., Jazayeri, S.D., Sedaghat, S., Shabanzadeh, P., Jahangirian, H., Mahdavi, M. & Abdollahi, Y. (2012). Synthesis and characterization of polyethylene glycol mediated silver nanoparticles by the green method. Int. J. Mol. Sci. 13(6), 6639–6650. DOI: 10.3390/ijms13066639.

30. Guo, F., Zhang, Q., Zhang, B., Zhang, H. & Zhang, L. (2009). Preparation and characterization of magnetic compo-

site microspheres using a free radical polymerization system consisting of DPE. Polym. Phy. 50, 1887–1894. DOI: 10.1016/j.polymer.2009.02.023.

31. Wang, B., Wei, Q., Qu, S.H. (2013). Synthesis and characterization of uniform and crystalline magnetite nanoparticles via oxidation-precipitation and modified co-precipitation metod. Int. J. Electrochem. Sci. 8, 3786–3793.

32. Mandal, M., Kundu, S., Ghosh, S.K., Panigrahi, S., Sau, T.K., Yusuf, S.M. & Pal, T. (2005). Magnetite nanoparticles with tunable gold or silver shell. J. Coll. Interf. Sci. 286(1), 94–187. DOI: 10.1016/j.jcis.2005.01.013.

33. Ge, Y., Zhang, Y., He, S., Nie, F., Teng, G. & Gu, N. (2009). Fluorescence modified chitosan-coated magnetic nanoparticles for high-efficient cellular imaging. Nanoscal. Res. Lett. 4(4), 287–295. DOI: 10.1007/s11671-008-9239-9.

34. Prucek, R, Tuček, J., Kilianová, M., Panáček, A., Kvítek, L., Filip, J., Kolář, M., Tománková, K. & Zbořil, R. (2011). The targeted antibacterial and antifungal properties of magnetic nanocomposite of iron oxide and silver nanoparticles. Biomaterials 32(21), 4704–4713. DOI: 10.1016/j.biomaterials.2011.03.039.

35. Sondi, I. & Salopek-Sondi, B. (2004). Silver nanoparticles as antimicrobial agent: a case study on E. coli as a model for Gram-negative bacteria. J. Coll. Interf. Sci. 275(1), 177–182. DOI: 10.1016/j.jcis.2004.02.012.

36. Morones, J.R., Elechiguerra, J.L., Camacho, A., Holt, K., Kouri, J.B., Ram, J.T. & Yacaman, M.J. (2005). The bactericidal effect of silver nanoparticles. Nanotechnology 16(10), 2346–2353. DOI: 10.1088/0957-4484/16/10/059.

37. Pal, S., Tak, Y.K. & Song, J.M. (2007). Does the antibacterial activity of silver nanoparticles depend on the shape of the nanoparticle? A Study of the gram-negative bacterium Escherichia coli. Appl Environ Microbiol. 73(6), 1712–1720. DOI: 10.1128/AEM.02218-06.